CrossMark

ORIGINAL PAPER

Phosphorus in water dispersible-colloids of forest soil profiles

Anna Missong · Roland Bol · Volker Nischwitz ·
Jaane Krüger · Friederike Lang · Jan Siemens ·
Erwin Klumpp

Abstract

Background and aims Nanoparticles and colloids affect the mobilisation and availability of phosphorus for plants and microorganisms in soils. We aimed to give a description of colloid sizes and composition from forest soil profiles and to evaluate the size-related quality of colloids for P fixation.

Methods We investigated the size-dependent elemental composition and the P content of water-dispersible colloids (WDC) isolated from five German (beech-dominated) forest soil profiles of varying bulk soil P content by field-flow fractionation (FFF) coupled to various detectors.

Results Three size fractions of WDC were separated: (i) nanoparticles <25 nm (NP) rich in C_{org}, (ii) fine colloids (25 nm–240 nm; FC) composed mainly of C_{org}, Fe and Al, probably as associations of Fe- and Al- (hydr)oxides and organic matter, and (iii) medium-sized colloids (240 nm–500 nm; MC), rich in Fe, Al and Si, indicating the presence of phyllosilicates. The P concentration in the overall WDC was up to 16 times higher compared to the bulk soil. The NP content decreased with increasing soil depth while the FC and MC showed a local maximum in the mineral topsoil due to soil acidification, although variant distributions in the subsoil were observed. NP were of great relevance for P binding in the organic surface layers, whereas FC- and MC-associated P dominated in the Ah horizon.

Conclusion The nanoparticles and colloids appeared to be of high relevance as P carriers in the forest surface soils studied, regardless of the bulk soil P content.

Responsible Editor: Phil Haygarth.

A. Missong (✉) · R. Bol · E. Klumpp
Institute of Bio- and Geosciences (IBG-3) Agrosphere,
Forschungszentrum Jülich, Wilhelm-Johnen-Str, 52425 Jülich,
Germany
e-mail: a.missong@fz-juelich.de

V. Nischwitz
Central Institute for Engineering, Electronics and Analytics,
Analytics (ZEA-3), Forschungszentrum Jülich, Wilhelm-Johnen
Str, 52425 Jülich, Germany

J. Krüger · F. Lang
Faculty of Environment and Natural Resources, Chair of Soil
Ecology, University of Freiburg, Bertoldstr. 17, 79098 Freiburg
i.Br, Germany

J. Siemens
Institute for Soil Science and Soil Conservation, iFZ Research
Centre for Biosystems, Land Use and Nutrition, Justus Liebig
University Giessen, Heinrich-Buff-Ring 26-32, 35392 Gießen,
Germany

Abbreviations

NP	Nanoparticles
FC	Fine colloid
MC	Medium colloid
WDC	Water-dispersible colloids
OM	Organic matter
BBR	Bad Brückenau

VES	Vessertal
MIT	Mitterfels
CON	Conventwald
LUE	Lüss
ICP-MS	Inductively coupled plasma mass spectrometry
FFF	Field-flow fractionation
DLS	Dynamic light scattering
UV	Ultraviolet
OCD	Organic carbon detector

Introduction

Phosphorus (P) is one of the nutrients controlling forest growth and vitality. Generally, for plants and microorganisms the soil represents the major source of phosphorus-containing compounds, in particular orthophosphate and organo-phosphorus forms, in such ecosystems. During ecosystem succession and soil development, the binding forms in which P is stored change systematically (Walker and Syers 1976). During bedrock weathering and pedogenetic development, P is released as phosphate (PO_4^{3-}) from primary minerals (such as apatite) or from secondary soil minerals. Phosphate can be taken up by biota and can thus be transformed into organic P compounds. Phosphate can be sorbed to soil minerals, mostly Fe- and Al-(hydr)oxides, (McDowell et al. 2007; Walker and Syers 1976), or bound to soil organic matter (OM), with cations such as Al^{3+} acting as bridging agents between the phosphate and OM (Borie and Zunino 1983). Biodegradable organic-P forms remain in the OM, and can be associated (adsorbed, complexed, co-precipitated) with soil particles such as metal(hydr)oxides and phyllosilicates (Celi and Barberis 2005; Ognalaga et al. 1994) or mineralised to PO_4^{3-} (Turner et al. 2007). The different transformations and storage options of P forms greatly depend on the soil moisture (Meier and Leuschner 2014), and microbial community (Bergkemper et al. 2016), vegetation type and cover, as well as on soil chemistry and mineralogy (Giesler et al. 2004). With increasing soil age, larger proportions of P compounds are transformed into P forms associated with soil minerals, or are lost from the ecosystems via leaching or surface runoff (Bol et al. 2016).

Natural soil nanoparticles (diameter d < 100 nm) and colloids (d < 1000 nm) represent the small particulate phase of soils. They consist of secondary minerals resulting from weathering of soils, or of natural OM, or are formed by aggregation of these inorganic and organic soil compounds (Hartland et al. 2013; Tsao et al. 2011). Typically, the colloidal soil fraction is rich in Fe- and Al-(hydr)oxides and phyllosilicates. Due to their small size and large specific surface, colloids are able to bind larger proportions of nutrients such as P per mass unit in comparison to the bulk soil material and they are therefore commonly regarded as a reservoir of sorbed P (Cross and Schlesinger 1995; Schoenau et al. 1989; Tiessen et al. 1984). Colloidal-associated inorganic or organic P can be sorbed onto or incorporated in colloidal-sized aggregates (Jiang et al. 2015a; Regelink et al. 2015a) and possibly nano Al- or Fe-P phases are formed. Furthermore, Liu et al. 2014 demonstrated the possible formation of nanoscale hydroxyapatite as a part of colloidal P in agricultural soils. Previous studies showed that natural soil nanoparticles and colloids play a major role in P cycling (Gottselig et al. 2014; Haygarth et al. 1997; Hens and Merckx 2001; Ilg et al. 2008; Jiang et al. 2015b; Liu et al. 2014; Siemens et al. 2004), and are important for the transport of P in soils (Bol et al. 2016; Holzmann et al. 2016; Jiang et al. 2017; Rick and Arai 2011; Wilkinson and Lead 2006). The formation (Tsao et al. 2011) and potential mobilisation of natural nanoparticles and colloids from soils depend on soil physical properties such as moisture, temperature and soil chemical parameters, such as pH and ionic strength (Jiang et al. 2013; Klitzke and Lang 2009; Klitzke et al. 2012; Tsao et al. 2011). Moreover, additional studies found that especially organic P is associated with the water-dispersible soil colloids (WDC) (Celi and Barberis 2005; Jiang et al. 2015b; Missong et al. 2016; Vincent et al. 2012). Other recent studies highlighted that in stream waters large proportions of P are associated with nanoparticles and colloids, and their origin was assumed to be linked to soil colloids released into the stream (Gottselig et al. 2014; Gottselig et al. 2017a). For these reasons, colloidal associated P is assumed to play a major role in P mobilisation, P leaching and ultimately soil P losses which urgently needs to be investigated and quantified (Bol et al. 2016). However, detailed chemical and size related characterisations of naturally formed soil colloids are rare, although they are fundamental for further investigating the role of such colloids for P mobilisation, leaching and losses. The

WDC are the finest soil fraction that can be extracted from a soil by water. The WDC represent only a minor proportion of the bulk soil, and although they are relatively enriched with P, they typically still represent overall only a small proportion of the bulk soil P (Bol et al. 2016). However, they represent the colloidal P pool that potentially can be mobilised, translocated and finally lost. Thus, due to their relatively large P content compared to the bulk soil, a large proportion of soil P can be leached in a colloidal form (Holzmann et al. 2016). Different types of WDC have been identified for soil horizons, in particular when comparing colloids extracted either from the organic layers or from mineral soils (Klitzke and Lang 2009; Schumacher et al. 2005; Sequaris et al. 2013). The type and the pedogenetic state of a natural soil appear to be crucial factors for colloid formation and therefore for the binding and storage of P. As an example, an enhanced formation of P-bearing Fe- and Al-(hydr)oxides in illuvial-horizons of the mineral soil is a typical pedogenetic effect of podzolisation in acidic forest soils (Jansen et al. 2003). However, an increased content of Fe- and Al-(hydr)oxides in acidic mineral Ah horizons compared to the organic layers will enhance the binding of P to the particulate phase and thereby counteracts vertical losses of inorganic and organic P (mostly dominated by phytate) from the organic layers by promoting P retention via effective sorption (Kaiser 2001). Recent literature studies have characterized WDC (Jiang et al. 2015b; Regelink et al. 2013, 2014, 2015b) according to their association with P. However, little is known about the soil nanoparticles and colloids in non-agricultural soils such as forest soils and detailed information regarding their role for P binding is scarce.

Field-flow fractionation coupled online to various detectors, including inductively coupled plasma mass spectrometry (ICP-MS), an organic carbon detector (OCD), an ultra-violet (UV) detector and dynamic light scattering (DLS), was used for the size separation of natural colloidal particles (Gottselig et al. 2014; Regelink et al. 2013; von der Kammer et al. 2011). The study presented here compared the soil profiles of five German forests located in low mountain range areas with similar vegetation and climate (Table 1), but different soil P concentrations. The objective was to examine the following issues: i) What type of water-dispersible nanoparticles and colloids can be found in forest soils using FFF? ii) How are the different kinds of water-dispersible nanoparticles and colloids distributed over the soil depth? iii) How is P distributed across the different types of nanoparticles and colloids and which types contain most P? iv) Does the WDC content and the distribution of P across the different types of nanoparticles and colloids, change with increasing bulk soil P content of the five soils studied?

Materials and methods

Forest test sites

The sampling sites were Bad Brückenau (BBR), Vessertal (VES), Mitterfels (MIT), Conventwald (CON) and Lüss (LUE), located in the Rhön Mountains (BBR), Thuringia (VES), Bavarian Forest (MIT), Black Forest (CON), and German plain, Lower Saxony (LUE) areas respectively. All soil samples were taken from beech dominated plots, even though some forests are beech/spruce mixed forest (e.g. CON). All the forest soils are acidic Cambisols. The soil samples were taken as part of the DFG SPP project 1685 on ecosystem nutrients: forest strategies for limited phosphorus resources. The five forest sites cover a wide range of bulk soil P stocks with the P richest soils at BBR and the P poorest soils being present in LUE. Moreover, these sampling locations have similar climatic conditions and similar vegetation. More details about the test sites are given in Table 1.

The soil samples were collected from soil pits in a sampling campaign in autumn 2013. The individual humus layers (L, Of, Oh) were separated and sampled by hand. The mineral soils were sampled as 5 and 10 cm thick slices for horizons A and B, respectively, the total number of samples per horizon depending on the total thickness of each horizon. Soils were sampled down to a maximum depth of 1 m. Following this procedure, we obtained 10 (BBR), 13 (VES) 15 (MIT), 10 (CON) and 11 (LUE) different depth layers per site. An aliquot of around 100 g was cooled and stored in a fridge before extraction and analysis. Another aliquot of all the soil samples was homogenised by sieving <2 mm and analysed for soil texture, pH, soil nutrient concentrations (incl. C_{org}, oxalate and dithionite extractable Fe) as part of the DFG SPP 1685. These data which were used for comparison and correlation analysis were provided by Lang et al. (2017).

Table 1 Properties of the five forest sites. All test sites were part of the DFG SP project 1685 and are among to Level II low mountain ranges monitoring sites in Germany. The average bulk soil P contents of the organic layer (O), upper mineral (Ah) soil and mineral soil measured after HF digestion are given in µmol per gram soil. The pH was measured in mineral soil water extracts. The bulk soil data originated from Lang et al. 2017

Site	Bad Brückenau (BBR)	Vessertal (VES)	Mitterfels (MIT)	Conventwald (CON)	Lüss (LUE)
Mean annual temperature °C	5.8	5.5	4.5	6.8	8.0
Altitude m	809	810	1023	840	115
Mean annual Precipitation mm	1031	1200	1299	1749	779
Soil type (WRB 2015)	Dystric Skeletic Cambisol (Hyperhumic. Loamic)	Hyperdystric Skeletic Chromic Cambisol (Hyperhumic. Loamic)	Hyperdystric Chromic Folic Cambisol (Humic. Loamic. Nechic)	Hyperdystric Skeletic Folic Cambisol (Hyperhumic. Loamic)	Hyperdystric Folic Cambisol (Arenic. Loamic. Nechic. Protospodic)
Organiclayer	Mull-like Moder	Moder	Moder	Mor-like Moder	Mor-like Moder
Parent material	Basalt	Trachyandesite	Paragneiss	Paragneiss	Sandy till
Texture (topsoil) (WRB 2015)	Siltyclay loam	Loam	Loam	Loam	Loamy sand
Texture (subsoil) (WRB 2015)	Loam	Sandy loam	Sandy loam	Sandy loam	Sand
Bulk soilP content µmol g_{soil}^{-1} (HF- dig.)	O: 51 Ah: 101 B: 71	O: 43 Ah: 40 B: 36	O: 23 Ah: 34 B: 29	O: 30 Ah: 26 B: 15	O:25 Ah: 5 B:5

Extraction of water-dispersible colloids

The WDC were extracted based on the protocol of Sequaris and Lewandowski (2003). The field-fresh soils were sieved <2 mm immediately before WDC extraction. Field-fresh soil was suspended in deionised water (dispensed from a Millipore system) in a ratio of 1:2 (w:v) and shaken for 6 h on a horizontal shaker at 150 rpm. The suspension was diluted 4-fold with deionised water and left to sediment for approximately 10 min. Using a pipette the supernatant was decanted and the sediment fraction >63 µm and any floating soil material was removed. Subsequently the supernatant soil extract was centrifuged for 5 min at 4000 g to obtain the fraction smaller than 500 nm in the supernatant. We worked with the WDC < 500 nm to evaluate the nanoparticles and colloids. The centrifugation time for the definite particle size range was calculated according to Hathaway (1955). The supernatants, containing the WDC were removed with a pipette. The extraction procedure was controlled by offline dynamic light scattering (DLS) size measurements determined by particle mass. The DLS measurement confirmed maximum particle sizes of 500 nm and the highest intensity was measured at mean sizes of 250–300 nm in the supernatant. After extraction, all samples were analysed with FFF within one week. It should be noted that in comparison to deionised water, the amount of WDC is reduced at typical ionic strengths of soil solutions due to the compressed electrical double layer of the particles. However, in the case of precipitation events, the ionic strength temporarily decreases resulting in an enhanced release of colloids.

An aliquot (30–50 mL) of the supernatant of the soil suspension was centrifuged at 10000 x g, the remaining colloid-free electrolyte phase was decanted and the residue freeze-dried. The dried material was weighed to calculate the average colloid weight of the WDC-extracts of each forest soil horizon. An aliquot of each bulk soil sample (2–5 g) was dried at 55 °C to constant weight to calculate the gravimetric soil moisture. All soil data were corrected for moisture and reported as µmol of the analyte per gram dry soil.

The WDC extraction procedure showed an uncertainty for the absolute WDC content of 10%. The relative element concentrations (ratios between the elements) were not affected by the absolute amounts of extracted colloids. The relative standard deviation of the organic C concentration (using OCD) for four measurements of a representative sample was calculated to be

2.5%. The limit of detection for organic C was 0.01 mg L^{-1}. The variation of the ICP–MS peak area for four measurements of a representative sample was calculated to be 4.6% for ^{31}P, 7.0% for ^{27}Al, 4.8% for ^{28}Si, 4.7% for ^{55}Mn, 6.3% for ^{43}Ca and 5.7% for ^{56}Fe. The limit of detection (calculated for the 200 μL injection volume) was 0.1 μg L^{-1} for P, 0.01 μg L^{-1} for Al, 3.3 μg L^{-1} for Si, 0.01 μg L^{-1} for Mn, 0.1 μg L^{-1} for Ca and 0.02 μg L^{-1} for Fe.

Field-flow fractionation

The nanoparticles and colloids were size separated using asymmetric field-flow fractionation (FFF; AF2000, Postnova Analytics, Landsberg, Germany). The FFF was coupled online to a UV-vis detector (Postnova Analytics), dynamic light scattering detector (DLS; Malvern Instruments), an organic carbon detector (OCD; DOC laboratory Dr. Huber, Germany) and an inductively coupled plasma mass spectrometer (ICP-MS; Agilent 7500, Agilent Technologies, Japan). The content of organic-C (C_{org}) (with OCD), phosphorus, iron (Fe), aluminium (Al), silicon (Si), calcium (Ca) and manganese (Mn) was determined in the WDC fractions. Further details of the FFF technique and analytical element determination are described elsewhere (Giddings 1993; Neubauer et al. 2011; Nischwitz et al. 2016; von der Kammer et al. 2011).

The parameters of the separation method are given in Table 2. Particle size resolution of the applied FFF separation was checked by analysing latex standards of the sizes 21 nm, 64 nm, 100 nm and 600 nm (from Postnova analytics) under the same conditions as the samples. Quantification using ICP-MS and OCD was undertaken via external multipoint calibration (4 to 8 concentration levels) and linear regression.

Data analyses

The raw data of the ICP-MS measurements were collected in counts per second (CPS) with the ICP-MS MassHunter Workstation Software (Agilent Technologies, Japan). The OCD raw data were collected in volts of the detector signal (V) with the AF^4 analytical software (Postnova, Landsberg, Germany). The raw data were exported to Excel® (Microsoft Corporation, Redmond, USA). The peak areas of the separated particle fractions were integrated and converted to the concentration (μM) by means of linear, multipoint

Table 2 Parameters and conditions for FFF separation

Parameter	
Membrane	PES (1 kDa)
Spacer	350 μm
Carrier solution	25 μM NaCl in deionised water
Detector flow	0.5 mL min^{-1}
Injection volume	200 μL
Injection flow	0.3 mL min^{-1}
Method	
Cross-flow$_1$	2.5 mL min^{-1}
t_0 - t_1 Focus time	12 min
t_1 - t_2 Transition time	1 min
t_3 - t_4 Constant flow	0.5 min
t_4 - t_5 Power mode (0.2 exponential)	20 min
Cross-flow$_2$	0.15 mL min^{-1}
t_5 - t_6 Power mode (0.8 exponential)	10 min
Cross-flow$_3$	0 mL min^{-1}
t_5 - t_6 Constant flow	30 min

calibration. Finally, the results were transformed into the unit μmol $g^{-1}_{dry\ soil}$ considering the water content of the samples and the extracted sample weight. The WDC content of the dry soil horizons was given in mg colloid per g soil.

Results

Size and composition of water-dispersible colloids

In general, the FFF fractograms (Fig. 1) showed a size-resolved separation of the nanoparticulate and colloidal fractions of the soil WDC-extracts. The online detection of the UV- and OCD-signals and the online measurements with DLS and ICP-MS provided complementary information about the colloidal size and composition. Three size fractions were separated for the WDC < 500 nm obtained from the forest soil extract (Fig. 1). The FFF fractograms of VES in Fig. 1 were chosen to exemplify the three size fractions present in the different soil horizons. The UV fractograms of WDC from all the sites are shown in Figs. S1-S5.

The first eluting peak of the fractograms represents the nanoparticulate soil fraction (NP) up to a size of 25 nm according to a size calibration based on
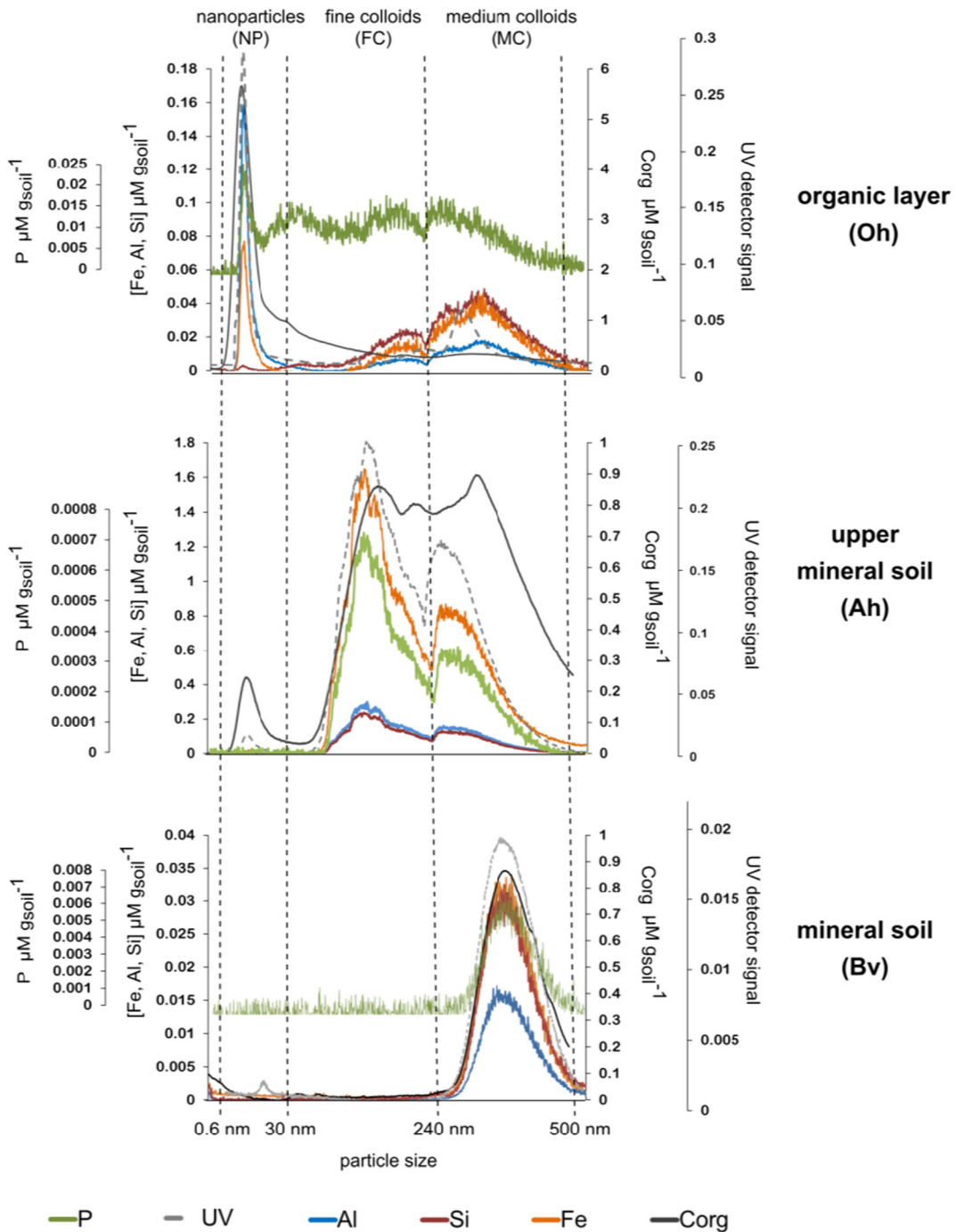
Fig. 1 FFF fractograms of WDC of three soil horizons of the soil profile VES. The FFF separation data shown were detected with ICP-MS (Fe, Al, Si, P concentration), UV and OC detectors. The y-axis scale is adapted to the detected concentration levels (given in μmol per g dry soil). The elution time scale of the x-axis was converted into a particle size scale segmented into three fractions. Special consideration should be given to the concentration scale on the y-axes

the analysis of latex standards. The second peak was assigned to the fine colloids (FC) in a size range from 25 nm to 240 nm. Finally, a third peak containing

medium-sized colloids (MC) with a size range between 240 nm and 500 nm was found based on DLS measurements. The MC fraction included particles of
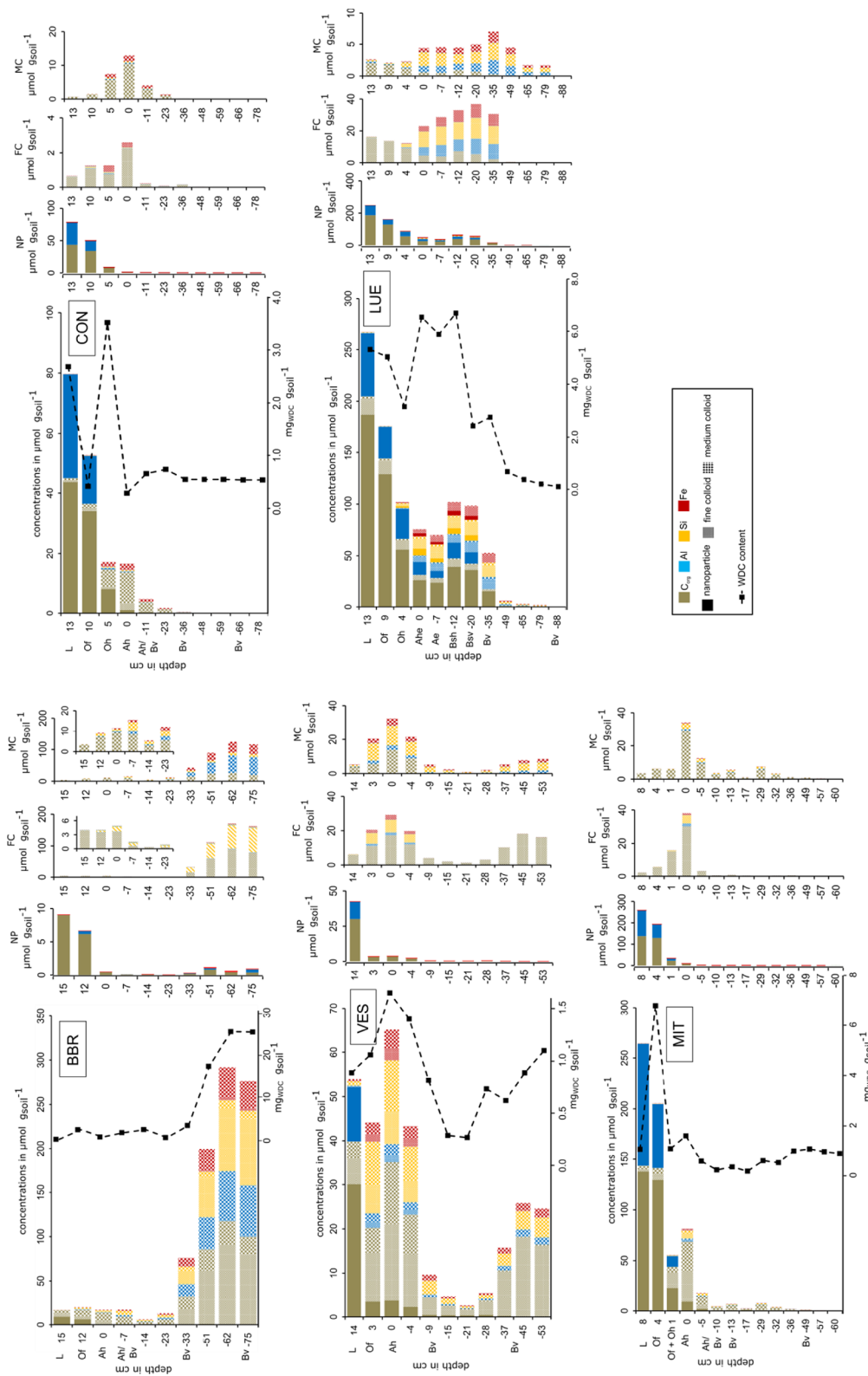
Fig. 2 Bar diagrams show the WDC element concentration (in μmol per g dry soil; element concentrations from the integrated peak area) of the three colloid fractions NP (complete filling), FC (hatched filling), MC (square filling) for C_{org}, Fe, Si and Al, the main components of the WDC. Data (also for Ca and Mn) are shown in Table S1 of the supplementary material. The NP, FC and MC depth distributions of P are shown in Fig. 4. The WDC content was calculated from the weight of freeze-dried WDC extracts (dashed line)

the "release peak", when the cross-flow was zero. The particles in the release peak are not perfectly separated by size (described by Neubauer et al. 2013). Nevertheless, the particles in this fraction have a minimum size of 240 and a maximum size of 500 nm.

The NP fractograms were characterised by intense UV (measured at 245 nm wavelength) and OCD-signals as shown in Fig. 1 for VES (only in the organic layer). The quantification of these signals (data in Table S1 and Fig. 2), indicated the dominance of OM in NP (see also Fig. 2, Table S1). Besides C_{org}, Al was predominantly detected in the first NP fractions (Figs. 1 and 2, Table S1 (NP)), but only small amounts of Fe (Table S1 and Fig. 2). The chemical composition of FC and MC were similar (Table S1, Fig. 2). The FC and MC contained C_{org}, Fe, Al, Si, Ca and P (Figs. 1 and 2, Table S1). However, the FC were characterised by a higher proportion of C_{org} (Figs. 1 and 2, Table S1).

WDC content and distribution in soil horizons

The WDC content differed between the soil horizons (Fig. 2). The WDC content in the organic layer and upper mineral soil was between 0.1–6.5 mg g^{-1}$_{dry\ soil}$; while in the subsoils the WDC contents were typically smaller with values ranging from 0.1–1 mg g^{-1}$_{dry\ soil}$. An exception was the soil from BBR, which showed much larger subsoil WDC concentrations than the other investigated soils of up to 25 mg g^{-1}$_{dry\ soil}$ (Fig. 2, Table S1). The distribution of the WDC in the soil profiles did not significantly correlate to the clay content of the soil material (Fig. S6), (clay content data reported in Lang et al. 2017).

Clearly, the element proportions varied for the NP, FC and MC of the five forest soils. Also for a given soil the elemental compositions of the WDC differed between the NP, FC, and MC. Actually, the element composition of, in particular FC and MC were similar for a given soil horizon, but differed between topsoil FC/MC and subsoil FC/MC (Figs. 1 and 2 and Table S1). The element compositions of the WDC in the soil horizons are described in detail in Fig. 2 starting from the topsoil and then moving downwards to the subsoil.

The NP fraction occurred predominantly in the Oh-layers and Ah-horizons and decreased by depth. The NP were largely present in the organic layer of BBR, VES, MIT and CON and even down to the Bsh horizon in the

podzol LUE. Organic C significantly contributed to all three size fractions and was present in the WDC of all horizons (Fig. 2). The C_{org} content of the colloids was largest in the organic layer of LUE, CON and MIT. Here the WDC-associated C_{org} concentrations (mainly present in the NP fraction) were around three times larger in the organic layer than in the WDC of the Ah and B horizon (FC and MC in Ah-, Ae-, Bsh-, Bsv-horizon; MC in the BV horizon). In the organic layer of LUE, CON and MIT, the NP made up the highest proportion of the WDC (Fig. 1, compare NP, FC, MC in Fig. 2 and Table S1) therefore the WDC in the organic layer were dominated by C_{org} and Al. In contrast, in BBR the WDC-C_{org} concentration was larger in the B horizon than in the organic layer and in VES the WDC-C_{org} concentrations of the B horizon were in the same order of magnitude as in the organic layer. But in VES and BBR subsoil the WDC-C_{org} was mainly present of the FC and MC.

The Fe, Si, Ca and Mn concentrations of the organic layer were around 10 times lower than in the Ah horizon. Nevertheless, also small signals of FC and MC were present in the organic layers and their relevance increased from litter to Oh layer. Under the organic layer, the proportion of NP rapidly declined and the relevance of the FC and MC fraction increased (Fig. 1, compare NP, FC, MC in Fig. 2 and Table S1). In
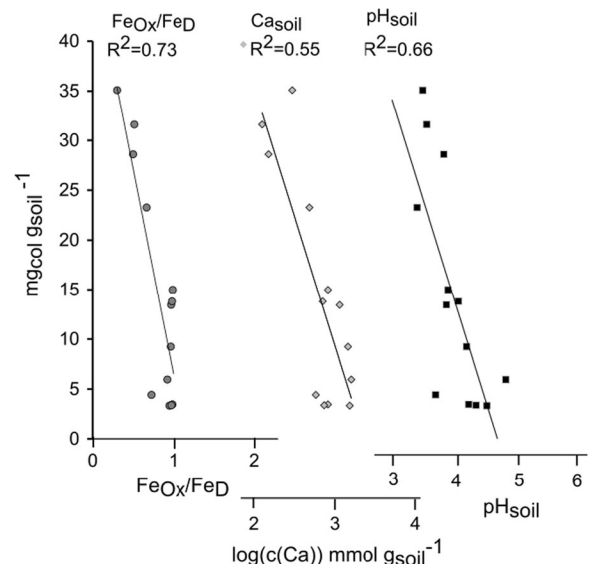

Fig. 3 Linear regressions between the WDC content in the surface soil (in mg$_{WDC}$ g^{-1}$_{dry\ soil}$) and the bulk soil parameters such as pH (p-value < 0.001), bulk Ca concentration (*p*-value < 0.005) and oxalate and dithionite extracted Fe (Fe_ox/Fe_D) (*p*-value < 0.001). Bulk soil data of the five forests from Lang et al. (2017)

addition to C_{org} the FC and MC also contained larger proportions of Fe, Ca, Mn, and Si than the NP.

The element contents of the MC and in particular of the FC fraction showed an increase in the Ah horizon of all forest soils in comparison to the organic layer. Also in the illuvial horizons Bsh and Bsv of LUE, the FC dominated the WDCs (Fig. 2, and Table S1). Therefore, a local WDC maximum occurred in the upper mineral soils of all five forests.

The FC and MC dominated the WDC in the mineral topsoil and were composed of C_{org}, Fe, Al and Si. However, the elemental proportions within the FC and MC fractions were different for the five forest soils (Fig. 2, Table S1). In LUE the topsoil FC and MC had comparable proportions of Al, Fe and Si (Fig. 2). In contrast the FC and MC were dominated by C_{org} of the mineral topsoil from BBR. The CON site had low WDC contents in the topsoil and the FC and MC contained besides C_{org} mainly Fe. In this mineral topsoil zone, the LUE soil displayed the highest WDC content with values of about 6 mg_{WDC} $g^{-1}_{dry\ soil}$. In contrast, BBR, VES and MIT had much lower WDC contents of 0.5–3 mg_{WDC} $g^{-1}_{dry\ soil}$ in the mineral topsoil (Fig. 2, Table S1). The WDC content of the mineral topsoil samples significantly increased with decreasing pH, decreasing ratio between oxalate and dithionite-extractable Fe and decreasing total Ca content (Fig. 3).

In the five forest subsoils, the WDC content per gram soil and the associated concentrations of elements in the WDC fractions showed different trends.

In the B horizons of MIT, CON and LUE, only low amounts of the MC fractions were present and decreased with increasing depth (Fig. 2 Table S1). Since it was the dominant WDC fraction, also the total WDC content decreased with increasing depth at these sites. In contrast, in the subsoil of BBR and VES, the WDC content increased. In BBR, the content of elements associated with WDC in the B-horizon was larger than in the Ah-horizon (Fig. 2, Table S1). In these subsoils, MC and also FC were present, although their elemental composition was different from the FC in the mineral topsoil (Fig. 2, Table S1).

Phosphorus association with WDC

The high specific surface area of the WDC typically leads to an enrichment of nutrients within the WDC fraction in comparison to the bulk soil. Phosphorus was 2- to16-fold enriched in the WDC in comparison to the bulk soil. The WDC content was highest for BBR (subsoil) and LUE (Ae, Bsh, Bsv) illustrating that the extractable colloid contents do not relate to the bulk soil P concentrations (shown in Table 1) since BBR is the forest with the highest P content and LUE the forest site with the lowest. The average P saturation ratios as calculated from the elemental concentrations according to the eq. (P/(0.5 x (Fe + Al))) (Leinweber et al. 1997) of the mineral bulk soil (A and B horizon) were 0.01 for LUE, 0.02 for CON, 0.04 for MIT, 0.05 for BBR, and
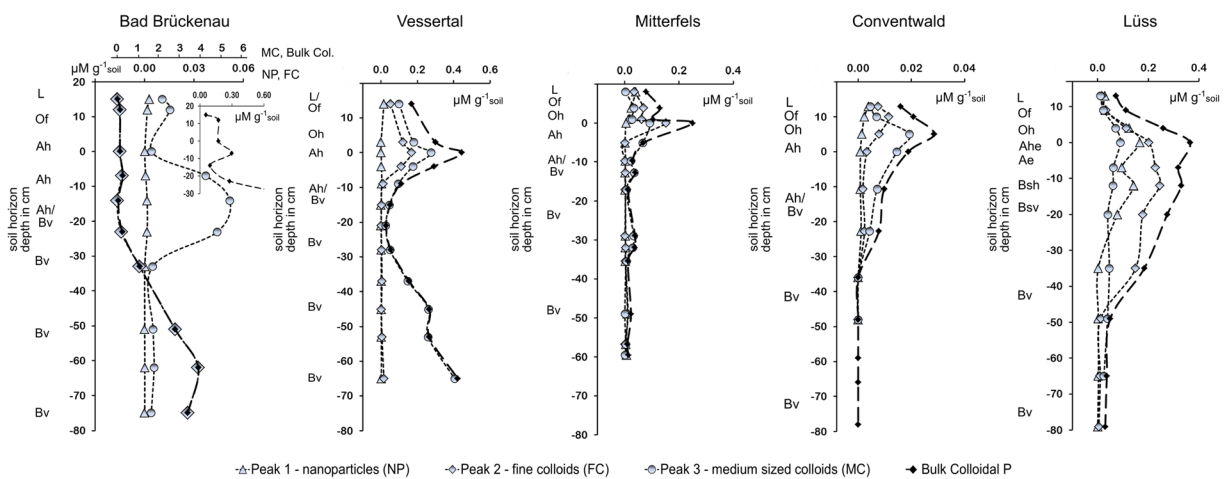

Fig. 4 WDC-P content in the soil depth profiles of the five sampling test site profiles. The scales of the x-axes vary due to adaptation to the respective concentrations of the samples (given in $\mu mol\ g^{-1}_{dry\ soil}$). The WDC-P content of the CON was below the detection limit in the deeper B-horizon

0.04 for VES. In comparison, the average P saturation ratios of the colloidal fractions were 1.5 to 11 times higher: 0.11 for LUE, 0.03 for CON, 0.19 for MIT, 0.15 for BBR and 0.13 for VES.

Although the WDC contents were relatively large in the organic layers, the WDC-associated P concentrations were rather small. For some WDC size fractions the WDC associated P concentration was close to the detection limit. In the organic layer, the NP constituted a maximum of 5% of the WDC-associated P (in MIT and LUE, Fig. 4, and Table S1). In the mineral soil horizons, nearly all the P was associated with the FC and MC. However, their importance for the P binding was different in the five Cambisols.

The local maximum of FC and MC content in the Ah and Ae horizons (and additionally the Bsh, Bsv horizons in LUE), (Fig. 2, Table S1) was accompanied by a local maximum of the WDC-associated P content (Fig. 4). In the (more) podzolised soil at LUE, the WDC-P, FC-P and MC-P concentrations decreased less sharply with increasing depths compared to those of the VES, MIT and CON profiles, in such a manner that concentrations greater than 0.3 µmol P g^{-1} were found in the Bsh and Bsv horizons. Therefore, the FC and MC contents of the upper mineral soil were of greatest relevance as a reservoir for WDC-associated P in the soil profile of all the five Cambisols. With increasing depth, the WDC content in LUE, CON and MIT decreased. However, in the subsoil, the MC fractions were still the main carrier of WDC-associated P (Fig. 2, Table S1, Fig. 4).

Discussion

Characteristics of the three WDC size fractions

The particles of the first peak in the fractograms (NP in Fig. 1) were identified as nanoparticles dominated by soil OM. Soil OM is rich in polar functional groups with the ability to complex metal ions such as Al^{3+} and Fe^{3+}. In the recent literature, Fe was often described as a component of nanoparticles <20 nm complexed by the OM or being present as an oxide, such as ferrihydrite (Baken et al. 2016; Gottselig et al. 2017b; Jiang et al. 2015a). The study by Gottselig et al. 2017a, b showed that the organic-dominated nanoparticles <20 nm from forest streams contained large amounts of Ca, Al and Fe. However, our data indicated that in the organic layer of the five investigated forest soils Al was clearly present

in the C_{org} dominated nanoparticles <25 nm, and only smaller concentrations of Fe and Mn were detectable (Fig. 2). The differences in NP composition between soils and streams may indicate some as yet unspecified alteration processes occurring during the transfer of NP from acidic forest soils to streams. The soil acidification in forest soils leads to the dissolution of Al(hydr)oxides to large extend. As a result the Al^{3+} is able to form associations with organic soil compounds as observed in our studies for the NP. Prietzel et al. 2016 reported the presence of Al-saturated soil OM in similar and comparable soils studied. In the subsoil the NP concentrations, in particular the NP- C_{org} concentrations decreased and the small NP signals were dominated by Fe, Mn and Si (Fig. 2, Table S1). The reasons for the large Al concentration in the NP of the organic layer WDC compared to the WDC of other soil studies (Jiang et al. 2013, 2015a, b; Regelink et al. 2013) or stream colloid analyses (Gottselig et al. 2014; Gottselig et al. 2017a, b; Baken et al. 2016) warrant further investigation about the C_{org}-forms present in NP and their affinity to associate with Al compared to Fe.

The elemental proportions of the FC and MC were different for the five forest soils, and the topsoil- and subsoil WDC of the same size showed different compositions regarding their proportions of Al, Si, Fe and C_{org}. The FC and MC composition was indicative of the metal(hydr)oxides (of Al, Fe and Mn), organic compounds and phyllosilicates, all which are typical of soil colloidal compounds (Tsao et al. 2011). These particles have different surface charges and thus are likely to form hetero-aggregates under acidic conditions. The organic carbon concentration found in the FC and MC fractions implied that organic compounds were likely to be associated with inorganic soil particles (Gottselig et al. 2017b; Kaiser et al. 2012). It appears that the FC and MC could be metal oxide colloids surrounded by OM or aggregates of these oxide-OM associations potentially also with phyllosilicates. Organic molecules as well as phosphate (Celi and Barberis 2005; Siemens et al. 2004) can modify the surface properties of colloids and stabilise them with respect to further aggregation to form larger particles and it also enhances their presence/extractability (Kretzschmar et al. 1995). In FFF studies on agricultural soils, it was also shown that fine colloids are mainly composed of Al- and Fe(hydr)oxides. They described WDC as consisting to a large extend of phyllosilicates, which were possibly coated with Fe oxides (Jiang et al. 2015b, 2017; Regelink et al. 2013).

Further corroboration was provided in FFF studies of nanoparticles and colloids from forest stream waters (Gottselig et al. 2014, 2017a), where the presence of Al- and Fe(hydr)oxides and phyllosilicates as fine colloids and their associates has also been reported.

WDC content and distribution across the five soil profiles

Conceivable reasons promoting the formation of soil colloids could be, for instance, the soil substrate composition (influencing the subsoil colloid formation) and the type of OM (related to the vegetation). Moreover, the chemical soil properties such as ionic strength or pH or the texture of the soils influence the quantity and type of WDC in a soil. The contents of extractable colloids differed greatly between the five forest soils and between soil horizons. Distinguishing the three fractions of the FFF provided further detailed clarity about the soil colloid types and composition. We found that the five investigated profiles showed a decrease of NP according topsoil depth and large FC and MC concentrations in the upper mineral topsoil. However, three groups could be distinguished comparing the distribution of the three size fractions along the profiles of the five forest soils. The first group included CON, LUE and MIT, here the proportion of NP was high in the organic horizon but the WDC concentration always decreased with depth. The sites BBR and VES represented two other distinct groups. At both sites the WDC content (dominated by FC and MC size fractions) increased again with depth in the B-horizon. However, VES showed high WDC concentrations in the topsoil whereas in BBR the WDC concentrations in the organic layer and topsoil were small in comparison to its subsoil. Specific soil properties explicit justifying the amount of WDC in the five forest sites, and explaining the distribution of the three fractions along the soil profile were not found. However, the reasons influencing the formation of colloids in a soil are diverse (Tsao et al. 2011). For instance the study by de Jonge et al. 2004 highlighted that the WDC content increased with increasing soil clay content. In contrast, our results showed that the WDC content of the five forest soils did not increase with the clay content of the bulk soils (Fig. S6). For instance, the mineral soils (A- and B-horizons) of the LUE test site displayed the lowest clay content but the highest WDC content, whereas VES or BBR showed high clay but low absolute WDC contents (Fig. S6). One

similarity of the LUE, CON and MIT soils is the ongoing podzolisation in these three forest sites (Werner et al. 2017), indicating that the podzolisation process had an influence on the formation of WDC, in particular for the NP in the organic layer of these forest soils. Moreover, our data indicates that the process of ongoing acidification in the mineral topsoil seem to have a large impact on the amount of extractable WDC in particular FC and MC. Additionally the co-presence of C_{org} and secondary soil minerals seem to have an impact on the amount and size of WDC. Therefore we expect the amount and size distribution of WDC in the five forest soils profiles is a coupled effect of various factors among others: C_{org} type and concentration, mineralogy, soil pH and clay content and their mutual impact. (Fig. 3).

WDC in the Oh- and Ah-horizons

The large proportion of NP in the organic layer of LUE, CON and MIT compared to BBR and VES cannot be attributed to one specific property. However, the relative proportion of Al in the NP of LUE, CON, and MIT was much larger than in the NP of BBR and VES. This can be indicative hint of the complexation of Al by OM as a key process forming NP at low pH. However, more detailed analysis of the OM functional groups may be needed to explain the formation of NP in organic forest soil layers.

The NP present in the organic layers occurred to a lesser extent in the mineral organic-rich Ah horizons (Fig. 1, Figs. S1-S5). In the mineral topsoil, the OM is more likely to form associations with the inorganic soil compounds, thereby potentially creating FC and MC. Therefore, the concurrent presence of organic compounds and inorganic soil minerals seem to be essential to form FC and MC in soils. The local maximum of WDC (FC and MC) in the mineral topsoil seemed to be favoured by such soil chemical conditions and properties. Figure 3 shows that the WDC contents (caused by the increased content of FC and MC) in the upper mineral soil increased with a decrease in the soil pH values, decreasing Ca content and increasing ratio between oxalate- and dithionite- extractable Fe. Also e.g. the work of Liang et al. (2010) showed that a pH decrease favours the colloid release. However, since the soil pH typically correlates with many different soil characteristics, it was hardly possible to unequivocally identify the factors controlling WDC formation. A decreasing topsoil Ca content and increasing ratio between oxalate- and

dithionite- extractable Fe with time of soil development are typical pedogenetic features that are linked to the ongoing acidification of soils, thereby leading to the formation of Cambisols and ultimately podzols on the parent rock materials we investigated. Furthermore, the increasingly acidic conditions in the topsoil increase the positive surface charge of the metal(hydr)oxides thereby promoting the binding of organic (and P) compounds, which could in turn have promoted the formation of WDC, especially of FC and MC. In addition, acidic conditions generally encourage the formation of soil aggregates between inorganic and organic compounds (Al-Kaisi et al. 2014; Kalbitz et al. 2005).

WDC in the B-horizon

As mentioned above, the depth distribution of WDC contents fundamentally differed between BBR and VES (WDC increased with depth) and CON, MIT, and LUE (WDC decreased with depth). However, we did not find any significant correlation between the subsoil WDC content and bulk soil chemical parameters. Soils at sites BBR and VES originate from a basaltic and andesitic substrates (Table 2) which are both basic rocks, rich in mafic minerals. In comparison, MIT and CON originated from gneissic bedrocks (acidic rocks) mainly consisting of quartz. The podzol LUE developed from quartz-rich fluvioglacial sand. Potentially the type and stage of weathering and secondary mineral assembly of the different rock types were the decisive factors determining WDC content in the subsoil. At sites VES and BBR, however, even though the bulk soil C_{org} content was low in all subsoils, a great proportion of the FC in the subsoil was composed of C_{org} and also the subsoil MC contained $C_{org.}$ Thus, OM was identified as important building block of WDC and potential driver of WDC formation not only in organic surface layers but also in underlying mineral soil horizons.

In LUE, and to a lesser extent in MIT, concentrations of C_{org}, Fe and Al of WDC decreased less rapidly with increasing soil depth compared to VES and CON sites (Figs. 1 and 2, Table S1). The LUE soil showed an illuvial horizon due to podzolisation (Table 2, Fig. 2, Table S1). In the illuvial Bsh and Bsv horizons of LUE, the FC (metal(hydr)oxide-rich) fraction dominated the WDC content. For the soil of LUE, and to lesser extent MIT, the study by Werner et al. 2017 also showed a zone of Al- and Fe- mineral enrichment in the depth range of the eluvial horizon which they interpreted to be the

result of mineral transfer due to podzolisation. Moreover, they showed a depletion of P and Fe in the deeper subsoil of LUE, MIT and CON, comparable to our WDC and WDC associated P findings. It is a hint that the local-maximum of WDC-associated P is related to the processes generating the metal-oxide formation. Hence, for WDC-associated P we support the suggestion that in LUE, and to lesser extent in MIT and CON, the P present in the B horizon originates from the soil surface. In addition, also Gangloff et al. (2014) analysed water-extractable organic carbon from acidic forest soils in which they reported an increase of water-extractable Fe and C (and P) at 20–30 cm soil depth (in the illuvial horizon) when compared to the topsoil. These authors assumed that nanoparticles could be responsible for the observed increase in the water-extractable concentrations of these elements.

Moreover, the BBR subsoil had a high proportion of clay and sesquioxide content compared to the other four soils. Such minerals are known to form the basis of inorganic soil colloids (Tsao et al. 2011) and probably therefore the FC and MC content increased with depth. This might indicate a continuous formation of soil colloids from the parent material, which then also bind P compounds. Moreover, Prietzel et al. 2016 showed for P binding in the BBR subsoil that the relevance of aluminium-saturated soil OM is high. In addition, they highlighted the fact that BBR subsoil contained Fe-P and Al-P minerals and apatite in the deeper substrate. Accordingly we also found high Al and C_{org} concentrations in the BBR subsoil WDC and potentially apatite or Fe-P or Al-P forms could also be present in the colloidal size class, which could explain the increase in P with soil depth. However, at VES, the sesquioxide content and clay proportion was in the same order of magnitude as that of MIT and CON (Lang et al. 2017), and therefore it cannot be the only reason for the observed WDC increase by depth in our study. Since VES soils were formed from basic soil substrate it is conceivable that the colloidal P forms are comparable to those of BBR. Therefore, the increasing contents of WDC-bound P with increasing depth at BBR and VES suggest that the primary release of P during weathering is likely to be an important, perhaps even the predominant, source.

Relevance of the three size fractions for P

The WDC size fractions of the five forest Cambisols were always enriched in P compared to the bulk soils.

This confirmed the high affinity of P to soil nanoparticles and colloids (Rick and Arai 2011). The important role of nanoparticulate and colloidal Fe- and Al-(hydr)oxides for P adsorption was also illustrated by their higher P-saturation ($P/(0.5*(Fe + Al))$) exceeding the P-saturation of the corresponding bulk soil samples. The acidic soil conditions in the forest soils favoured P sorption, especially to Fe-(hydr)oxides. Sorption and presence of ortho-P or inositol-P on Fe-(hydr)oxides has been shown to favour the dispersion and mobilisation of these colloids from bulk soil samples in laboratory experiments (Ilg et al. 2008). However, we found no significant correlation between the P saturation of the WDC and the amount of WDC in the forest soils. Also, the amount of WDC did not follow the bulk soil P gradient. The P-poor end of the gradient was the forest site LUE, whereas BBR had the largest soil P concentrations (Table 1). However, LUE and BBR displayed similar WDC contents in the O layer and the B horizon, and the largest WDC contents were found in the P-poor Ah horizon from LUE. Therefore, the bulk soil P content did not have an effect on the amount of WDC at our study sites.

The NP-associated proportion of P was large at the P-poorer sites of LUE, CON, and MIT, and smaller at VES and BBR. Most likely, large fractions of NP-bound P at the LUE, CON, MIT sites were linked to large NP concentrations (built up by C_{org}) resulting in proportionally higher NP-P concentrations. Also the NP we found no indication that the distribution of P across the three WDC size fractions was affected by the bulk soil P content. In the NP fractions, the P could be present as P-contained in organic molecules (P_o) or as phosphate associated with OM. For instance, Al (and Fe) might be bridging agents for the fixation of P to the humic colloids (Gerke 2010). Moreover, the P_o or phosphate associated with nanoparticulate Al/Fe(hydr)oxides may also represent a part of the NP (Jiang et al. 2015b; a; Regelink et al. 2013). The relevance of NP-bound P was only of significance in the organic layer (Fig. 2, Table S1). However, P was also significantly associated with the FC and MC in the organic layer. Assuming that organic NP can be transported more easily than FC and MC due to their smaller size, the role of NP for the potential P mobilisation from the organic layer is important, even though the FC and MC contained higher proportions of P compared to the NP (Fig. 4).

The local maximum of FC and MC in the forest topsoil also brings about the increase of WDC associated P. In the upper mineral soil, the P was mainly associated with the FC and MC. In the FC and MC fractions, we expect a fixation of phosphates and P_o to the metal(hydr)oxides and an association of metal(hydr)oxides and OM, in line with results from Jiang et al. 2015a, b and Missong et al. 2016. As shown in literature, P and soil OM can be incorporated into small soil aggregates (Jiang et al. 2015a, b; Wang et al. 2014; Werner et al. 2017). The OM and the P_o associated interior of the soil aggregates is sterically protected against plant uptake (Lützow et al. 2006). In general the P present in the colloids and colloidal sized aggregates is potentially more stable with respect to plant uptake or mineralisation compared to dissolved P. Therefore, we expect FC and MC as important P backup in the forest topsoil for plant-available P. The P in the topsoil may originate from the soil OM present in the upper mineral soil or may possibly be P leached from the organic layer. Kaiser (2001) described the mineral soil as a barrier for vertical P losses from organic layers by promoting P retention through an effective P sorption. Following this approach, the high content of P associated with the WDC in the Ah horizon of the forest soils (and the illuvial horizon in LUE) could be the result of the sorption and retention fixation of leached P (nanoparticulate associated or dissolved). We suspect that the upper mineral horizon acts as a zone of enhanced colloid formation and effective P sorption. However, the upper mineral soil is not a totally impassable barrier for dissolved or colloidal P leaching. It should also be mentioned that the majority of colloids (and dissolved compounds) transferred in soils are leached downwards in the soil profile through macropores or preferential flow paths (Jacobsen et al. 1997, Julich et al. 2017). Therefore, the soil structure related to soil density and the root penetration will significantly affect the vertical transfer of colloids. Indeed, due to the high content of FC and MC-associated P, further favoured by the topsoil acidification, they are likely to play an important role in the mobilisation of P from the surface soil. However, the WDC analyses produce a set of static data limiting its validity for colloid-associated P transfer. The concept of intensive mobilisation of colloid-associated P from the surface soil warrants further examination in future studies, also in the light of a lack of overall information on colloidal P fluxes in forest ecosystems (Bol et al. 2016). Furthermore,

in the deeper soil horizons, it remains uncertain which quantitative proportion of colloid-bound P was translocated from the Ah-horizon and which proportion one originated from the bedrock, because we could not distinguish the specific inorganic particle type with which P was associated. Indeed it remains an open question to which fraction of WDC in mineral soil horizons is formed autochthonously in situ and which is formed allochthonously (e.g. in organic surface layers).

Conclusion

Water-extractable nanoparticles and colloids in the investigated forest soils (Cambisols) can be separated by field-flow fractionation into three size fractions: nanoparticles (<25 nm), fine colloids (25 nm–240 nm) and medium colloids (240 nm–500 nm). The nanoparticles are rich in organic carbon and Al, while the fine and medium-sized colloids are associations between inorganic soil constituents (i.e., metal(hydr)oxides and phyllosilicates) and OM. In the organic layer, the nanoparticles <25 nm are the dominant WDC fraction. In the mineral topsoil, the content of fine and medium colloids was larger compared to the organic layer and the subsoil providing a local WDC maximum. The co-presence of highly weathered mineral soil and OM seem to be favourable for colloid formation. The local WDC maximum was found to be correlated to soil properties (pH, Ca content, ratio of oxalate-extractable-Fe:dithionite-extractable-Fe) affected by soil acidification. It was shown that WDC are important P-carriers in forest soils, containing significantly more P per mass unit than the bulk soil. In the organic surface layers, the organic-matter-dominated NP were important WDC associated P carriers but in the mineral soil horizons, fine and medium-sized colloids were the dominant WDC associated P carriers. Therefore, all three fractions of WDC are important potential sources and carriers of P in forest soils. However, enrichment of P in the WDC fraction and the WDC associated P concentration was not related to the bulk soil P content. The WDC preferentially consist of OM and P, thus they may be "hot soil components" for microorganisms and plants.

References

Al-Kaisi MM, Douelle A, Kwaw-Mensah D (2014) Soil microaggregate and macroaggregate decay over time and soil carbon change as influenced by different tillage systems. J Soil Water Conserv 69:574–580. https://doi.org/10.2489/jswc.69.6.574

Baken S, Regelink IC, Comans RNJ, Smolders E, Koopmans GF (2016) Iron-rich colloids as carriers of phosphorus in streams: A field-flow fractionation study. Water Res 99:83–90. https://doi.org/10.1016/j.watres.2016.04.060

Bergkemper F, Scholer A, Engel M, Lang F, Kruger J, Schloter M, Schulz S (2016) Phosphorus depletion in forest soils shapes bacterial communities towards phosphorus recycling systems. Environ Microbiol 18:1988–2000. https://doi.org/10.1111/1462-2920.13188

Bol R, Julich D, Brödlin D, Siemens J, Kaiser K, Dippold MA, Spielvogel S, Zilla T, Mewes D, von Blanckenburg F, Puhlmann H, Holzmann S, Weiler M, Amelung W, Lang F, Kuzyakov Y, Feger K-H, Gottselig N, Klumpp E, Missong A, Winkelmann C, Uhlig D, Sohrt J, von Wilpert K, Wu B, Hagedorn F (2016) Dissolved and colloidal phosphorus fluxes in forest ecosystems—an almost blind spot in ecosystem research. J Plant Nutr Soil Sci 179:425–438. https://doi.org/10.1002/jpln.201600079

Borie F, Zunino H (1983) Organic matter-phosphorus associations as a sink in P-fixation processes in allophanic soils of Chile. Soil Biol Biochem 15:599–603 https://doi.org/10.1016/0038-0717(83)90056-1

Celi LA, Barberis E (2005) Abiotic Stabilization of Organic Phosphorus in the Environment. In: BL Turner, E Frossard, DS Baldwin (eds) Organic Phosphorus in the Environment. CABI Publishing, Wallingford, Oxfordshire

Cross AF, Schlesinger WH (1995) A literature- review and evaluation of the Hedley fractionation - applications of the biogeochemical cycle of soil phosphorus in natural ecosystems. Geoderma 64:197–214. https://doi.org/10.1016/0016-7061(94)00023-4

Gangloff S, Stille P, Pierret M-C, Weber T, Chabaux F (2014) Characterization and evolution of dissolved organic matter in acidic forest soil and its impact on the mobility of major and trace elements (case of the Strengbach watershed). Geochim Cosmochim Acta 130:21–41 https://doi.org/10.1016/j.gca.2013.12.033

Gerke J (2010) Humic (Organic Matter)-Al(Fe)-Phosphate Complexes: An Underestimated Phosphate Form in Soils and Source of Plant-Available Phosphate. Soil Sci 175:417–425. https://doi.org/10.1097/SS.0b013e3181f1b4dd

Giddings JC (1993) Retention (steric) inversion in Field-Flow-Fractionation - Practical implications in particle-size, density and shape analysis. Analyst 118:1487–1494. https://doi.org/10.1039/an9931801487

Giesler R, Satoh F, Ilstedt U, Nordgren A (2004) Microbially available phosphorus in boreal forests: Effects of aluminum

and iron accumulation in the humus layer. Ecosystems 7: 208–217. https://doi.org/10.1007/s10021-003-0223-z

Gottselig N, Bol R, Nischwitz V, Vereecken H, Amelung W, Klumpp E (2014) Distribution of Phosphorus-Containing Fine Colloids and Nanoparticles in Stream Water of a Forest Catchment. Vadose Zone J 13:1–11. https://doi.org/10.2136/vzj2014.01.0005

Gottselig N, Nischwitz V, Meyn T, Amelung W, Bol R, Halle C, Vereecken H, Siemens J, Klumpp E (2017a) Phosphorus Binding to Nanoparticles and Colloids in Forest Stream Waters. Vadose Zone J 16 (3)

Gottselig N, Amelung W, Bol R, Nischwitz V, Siemens J, Kirchner J, Vereecken H, Avila Castells A, Båth A, Batalla R, Blomkvist P, Estany D, Eugster W, Falgin C, Granger S, Hernandez Crespo C, Herrmann F, Jackson-Blake L, Keizer JJ, Knöller K, Laudon H, Laurila T, Lehner I, Lindroth A, Löfgren S, Ottosson Löfvenius M, Lohila A, MacLeod K, Martín Monerris M, Mölder M, Müller C, Nasta P, Paul-Limoges E, Pierret M-C, Pilegaard K, Romano N, Stähli M, Sebatià MT, Taberman I, Voltz M, Wendland F, Klumpp E (2017b) Natural nanoparticles and colloids in European forest stream waters and their role for phosphorus transport. Glob Biogeochem Cycles. https://doi.org/10.1002/2017GB005657

Hathaway JC (1955) Procedure for clay mineral analysis used in the sedimentary petrology laboratory of the US Geological Survey. Clay Miner Bull 3:9–13

Haygarth PM, Warwick MS, House WA (1997) Size distribution of colloidal molybdate reactive phosphorus in river waters and soil solution. Water Res 31:439–448. https://doi.org/10.1016/s0043-1354(96)00270-9

Hens M, Merckx R (2001) Functional characterization of colloidal phosphorus species in the soil solution of sandy soils. Environ Sci Technol 35:493–500. https://doi.org/10.1021/es0013576

Holzmann S, Missong A, Puhlmann H, Siemens J, Bol R, Klumpp E, von Wilpert K (2016) Impact of anthropogenic induced nitrogen input and liming on phosphorus leaching in forest soils. J Plant Nutr Soil Sci 179:443–453. https://doi.org/10.1002/jpln.201500552

Ilg K, Dominik P, Kaupenjohann M, Siemens J (2008) Phosphorus-induced mobilization of colloids: model systems and soils. Eur J Soil Sci 59:233–246. https://doi.org/10.1111/j.1365-2389.2007.00982.x

Jansen B, Nierop KGJ, Verstraten JM (2003) Mobility of Fe(II), Fe(III) and Al in acidic forest soils mediated by dissolved organic matter: influence of solution pH and metal/organic carbon ratios. Geoderma 113:323–340 https://doi.org/10.1016/S0016-7061(02)00368-3

Jiang C, Sequaris JM, Vereecken H, Klumpp E (2013) Diffusion-controlled mobilization of water-dispersible colloids from three German silt loam topsoils: effect of temperature. Eur J Soil Sci 64:777–786. https://doi.org/10.1111/ejss.12086

Jiang X-Q, Bol R, Willbold S, Vereecken H, Klumpp E (2015a) Speciation and distribution of P associated with Fe and Al oxides in aggregate-sized fraction of an arable soil. Biogeosciences 12:6443–6452

Jiang X-Q, Bol R, Nischwitz V, Siebers N, Willbold S, Vereecken H, Amelung W, Klumpp E (2015b) Phosphorus Containing Water Dispersible Nanoparticles in Arable Soil. J Environ Qual 44:1772–1781

Jiang X, Bol R, Cade-Menun BJ, Nischwitz V, Willbold S, Bauke SL, Vereecken H, Amelung W, Klumpp E (2017) Colloid-bound and dissolved phosphorus species in topsoil water extracts along a grassland transect from Cambisol to Stagnosol. Biogeosci 14:1153-1164. https://doi.org/10.5194/bg-14-1153-2017

de Jonge LW, Kjaergaard C, Moldrup P (2004) Colloids and colloid-facilitated transport of contaminants in soils: An introduction. Vadose Zone J 3:321–325

Julich D, Julich S, Feger KH (2017) Phosphorus in preferential flow pathways of forest soils in Germany. Forests. 8(1):19. https://doi.org/10.3390/f8010019

Kaiser K (2001) Dissolved organic phosphorus and sulphur as influenced by sorptive interactions with mineral subsoil horizons. Eur J Soil Sci 52:489–493. https://doi.org/10.1046/j.1365-2389.2001.00396.x

Kaiser M, Berhe AA, Sommer M, Kleber M (2012) Application of ultrasound to disperse soil aggregates of high mechanical stability. J Plant Nutr Soil Sci 175:521–526. https://doi.org/10.1002/jpln.201200077

Kalbitz K, Schwesig D, Rethemeyer J, Matzner E (2005) Stabilization of dissolved organic matter by sorption to the mineral soil. Soil Biol Biochem 37:1319–1331. https://doi.org/10.1016/j.soilbio.2004.11.028

von der Kammer F, Legros S, Larsen EH, Loeschner K, Hofmann T (2011) Separation and characterization of nanoparticles in complex food and environmental samples by field-flow fractionation. Trac-Trends in Analy Chem 30:425–436. https://doi.org/10.1016/j.trac.2010.11.012

Klitzke S, Lang F (2009) Mobilization of Soluble and Dispersible Lead, Arsenic, and Antimony in a Polluted, Organic-rich Soil - Effects of pH Increase and Counterion Valency. J Environ Qual 38:933–939. https://doi.org/10.2134/jeq2008.0239

Klitzke S, Lang F, Kirby J, Lombi E, Hamon R (2012) Lead, antimony and arsenic in dissolved and colloidal fractions from an amended shooting-range soil as characterised by multi-stage tangential ultrafiltration and centrifugation. Environ Chem 9:462–473. https://doi.org/10.1071/en12010

Kretzschmar R, Robarge WP, Amoozegar A (1995) Influence of natural organic-matter in colloid transport through saprolite. Water Resour Res 31:435–445. https://doi.org/10.1029/94wr02676

Lang F, Krüger J, Amelung W, Willbold S, Frossard E, Bünemann E, Kandeler E, Marhan S, Schulz S, Bergkemper F, Schloter M, Bauhus J, Nitschke R, Mikutta R, Guggenberger G, Polle A, Pena R, Prietzel J, Kaiser K, Rodionov A, Talkner U, Meesenburg H, von Wilpert K, Hölscher A, Dietrich HP, Chmara I (2017) Soil phosphorus supply controls P nutrient strategies of beech forest ecosystems in Central Europe Biogeochem in press. https://doi.org/10.1007/s10533-017-0375-0

Leinweber P, Lünsmann F, Eckhardt KU (1997) Phosphorus sorption capacities and saturation of soils in two regions with different livestock densities in northwest Germany. Soil Use Manag 13:82–89. https://doi.org/10.1111/j.1475-2743.1997.tb00562.x

Liang XQ, Liu J, Chen YX, Li H, Ye YS, Nie ZY, Su MM, Xu ZH (2010) Effect of pH on the release of soil colloidal phosphorus. J Soils Sediments 10:1548–1556. https://doi.org/10.1007/s11368-010-0275-6

Liu J, Yang J, Liang X, Zhao Y, Cade-Menun BJ, Hu Y (2014) Molecular Speciation of Phosphorus Present in Readily Dispersible Colloids from Agricultural Soils. Soil Sci Soc Am J 78:47–53. https://doi.org/10.2136/sssaj2013.05.0159

McDowell RW, Cade-Menun B, Stewart I (2007) Organic phosphorus speciation and pedogenesis: analysis by solution P-31 nuclear magnetic resonance spectroscopy. Eur J Soil Sci 58:1348–1357. https://doi.org/10.1111/j.1365-2389.2007.00933.x

Meier IC, Leuschner C (2014) Nutrient dynamics along a precipitation gradient in European beech forests. Biogeochemistry 120:51–69. https://doi.org/10.1007/s10533-014-9981-2

Missong A, Bol R, Willbold S, Siemens J, Klumpp E (2016) Phosphorus forms in forest soil colloids as revealed by liquid-state P-31-NMR. J Plant Nutr Soil Sci 179:159–167. https://doi.org/10.1002/jpln.201500119

Neubauer E, van der Kammer F, Hofmann T (2011) Influence of carrier solution ionic strength and injected sample load on retention and recovery of natural nanoparticles using Flow Field-Flow Fractionation. J Chromatogr A 1218:6763–6773. https://doi.org/10.1016/j.chroma.2011.07.010

Neubauer E, Schenkeveld WDC, Plathe KL, Rentenberger C, von der Kammer F, Kraemer SM, Hofmann T (2013) The influence of pH on iron speciation in podzol extracts: Iron complexes with natural organic matter, and iron mineral nanoparticles. Sci Total Environ 461:108–116. https://doi.org/10.1016/j.scitotenv.2013.04.076

Nischwitz V, Gottselig N, Missong A, Meyn T, Klumpp E (2016) Field flow fractionation online with ICP-MS as novel approach for the quantification of fine particulate carbon in stream water samples and soil extracts. J Anal At Spectrom 31:1858–1868. https://doi.org/10.1039/C6JA00027D

Ognalaga M, Frossard E, Thomas F (1994) Glucose-1-phosphate and myoinositol hexaphosphate adsorption mechanisms on goethite. Soil Sci Soc Am J 58:332–337

Prietzel J, Klysubun W, Werner F (2016) Speciation of phosphorus in temperate zone forest soils as assessed by combined wet-chemical fractionation and XANES spectroscopy. J Plant Nutr Soil Sci 179(2):168–185

Regelink IC, Koopmans GF, van der Salm C, Weng L, van Riemsdijk WH (2013) Characterization of Colloidal Phosphorus Species in Drainage Waters from a Clay Soil Using Asymmetric Flow Field-Flow Fractionation. J Environ Qual 42:464–473. https://doi.org/10.2134/jeq2012.0322

Regelink IC, Voegelin A, Weng L, Koopmans GF, Comans RNJ (2014) Characterization of colloidal Fe from soils Using Field-flow fractionation and Fe K-Edge X-ray absorption spectroscopy. Environ Sci Technol 48:4307–4316. https://doi.org/10.1021/es405330x

Regelink IC, Stoof CR, Rousseva S, Weng L, Lair GJ, Kram P, Nikolaidis NP, Kercheva M, Banwart S, Comans RNJ (2015a) Linkages between aggregate formation, porosity and soil chemical properties. Geoderma 247:24–37. https://doi.org/10.1016/j.geoderma.2015.01.022

Regelink IC, Weng L, Lair GJ, Comans RNJ (2015b) Adsorption of phosphate and organic matter on metal (hydr)oxides in arable and forest soil: a mechanistic modelling study. Eur J Soil Sci 66:867–875. https://doi.org/10.1111/ejss.12285

Rick AR, Arai Y (2011) Role of natural nanoparticles in phosphorus transport processes in ultisols. Soil Sci Soc Am J 75:335–347. https://doi.org/10.2136/sssaj2010.0124nps

Schoenau JJ, Stewart JWB, Bettany JR (1989) Forms and cycling of phosphorus in prairie and boreal forest soils. Biogeochemistry 8:223–237

Schumacher M, Christl I, Scheinost AC, Jacobsen C, Kretzschmar R (2005) Chemical heterogeneity of organic soil colloids investigated by scanning transmission X-ray microscopy and C-1s NEXAFS microspectroscopy. Environ Sci Technol 39:9094–9100. https://doi.org/10.1021/es050099f

Sequaris JM, Lewandowski H (2003) Physicochemical characterization of potential colloids from agricultural topsoils. Colloids Surf A Physicochem Eng Asp 217:93–99. https://doi.org/10.1016/s0927-7757(02)00563-0

Sequaris JM, Klumpp E, Vereecken H (2013) Colloidal properties and potential release of water-dispersible colloids in an agricultural soil depth profile. Geoderma 193:94–101. https://doi.org/10.1016/j.geoderma.2012.10.014

Siemens J, Ilg K, Lang F, Kaupenjohann M (2004) Adsorption controls mobilization of colloids and leaching of dissolved phosphorus. Eur J Soil Sci 55:253–263. https://doi.org/10.1046/j.1365-2389.2004.00596.x

Tiessen H, Stewart JWB, Cole CV (1984) Pathways of phosphorus tranformation in soils of differing pedogenesis. Soil Sci Soc Am J 48:853–858

Tsao TM, Chen YM, Wang MK (2011) Origin, separation and identification of environmental nanoparticles: a review. J Environ Monit 13:1156–1163. https://doi.org/10.1039/c1em10013k

Turner BL, Condron LM, Richardson SJ, Peltzer DA, Allison VJ (2007) Soil organic phosphorus transformations during pedogenesis. Ecosystems 10:1166–1181. https://doi.org/10.1007/s10021-007-9086-z

Vincent AG, Schleucher J, Grobner G, Vestergren J, Persson P, Jansson M, Giesler R (2012) Changes in organic phosphorus composition in boreal forest humus soils: the role of iron and aluminium. Biogeochemistry 108:485–499. https://doi.org/10.1007/s10533-011-9612-0

Walker TW, Syers JK (1976) The fate of phosphorus during pedogenesis. Geoderma 15:1–19. https://doi.org/10.1016/0016-7061(76)90066-5

Wang R, Balkanski Y, Boucher O, Ciais P, Peñuelas J, Tao S (2014) Significant contribution of combustion-related emissions to the atmospheric phosphorus budget. Nat Geosci 8(1):48–54

Werner F, Rene de la Heye T, Spielvogel S, Prietzel J (2017) Small scale spatial distribution of phosphorus fractions in soils from silicate parent material with differnet degree of podzolization. Geoderma 302:52–65

Wilkinson KJ, Lead JR (2006) Environmental Colloids and Particles: Behaviour, Separation and Characterisation, vol 10. John Wiley & Sons. https://doi.org/10.1002/9780470024539.ch1